Enhanced Infrared Magneto-Optical Response of the Nonmagnetic Semiconductor BiTeI Driven by Bulk Rashba Splitting

L. Demkó,[1,*] G. A. H. Schober,[2,3] V. Kocsis,[4] M. S. Bahramy,[5] H. Murakawa,[5] J. S. Lee,[2,†] I. Kézsmárki,[4] R. Arita,[2,5] N. Nagaosa,[2,5] and Y. Tokura[1,2,5]

[1]*Multiferroics Project, Exploratory Research for Advanced Technology (ERATO), Japan Science and Technology Agency (JST), c/o Department of Applied Physics, University of Tokyo, Tokyo 113-8656, Japan*

[2]*Department of Applied Physics, University of Tokyo, Tokyo 113-8656, Japan*

[3]*Institute for Theoretical Physics, University of Heidelberg, D-69120 Heidelberg, Germany*

[4]*Department of Physics, Budapest University of Technology and Economics and Condensed Matter Research Group of the Hungarian Academy of Sciences, 1111 Budapest, Hungary*

[5]*Cross-Correlated Materials Research Group (CMRG) and Correlated Electron Research Group (CERG), RIKEN Advanced Science Institute (ASI), Wako 351-0198, Japan*

(Received 4 May 2012; published 15 October 2012)

We study the magneto-optical (MO) response of the polar semiconductor BiTeI with giant *bulk* Rashba spin splitting at various carrier densities. Despite being nonmagnetic, the material is found to yield a huge MO activity in the infrared region under moderate magnetic fields (up to 3 T). Our first-principles calculations show that the enhanced MO response of BiTeI comes mainly from the intraband transitions between the Rashba-split bulk conduction bands. These transitions connecting electronic states with opposite spin directions become active due to the presence of strong spin-orbit interaction and give rise to distinct features in the MO spectra with a systematic doping dependence. We predict an even more pronounced enhancement in the low-energy MO response and dc Hall effect near the crossing (Dirac) point of the conduction bands.

DOI: 10.1103/PhysRevLett.109.167401 PACS numbers: 78.20.Ls, 71.70.Ej, 78.20.Bh, 85.75.−d

The spin-orbit interaction (SOI) plays a crucial role in the rapidly evolving field of spintronics [1–4]. The principal importance of SOI is in its ability to intrinsically couple the electron's spin with its orbital motion, and hence produce many novel phenomena such as the spin Hall effect [5] and spin galvanic effect [6]. In the presence of an external magnetic field, SOI can effectively mediate the interaction between photons and electron spins, thereby leading to interesting magneto-optical (MO) effects, e.g., nonlinear Kerr rotation [7], whereby the polarization plane of the linearly polarized light in reflection is rotated as a consequence of SOI.

In practice, most materials under a magnetic field exhibit a rather complicated MO response. This is because usually several energy bands are involved in the optical excitations, which, given that SOI is also at work, leads to a variety of highly overlapping interband and intraband optical transitions. The complexity of such spectra prevents a comprehensive understanding of the role of SOI on the MO response of the given materials using the available theoretical models. In contrast, semiconductors with Rashba-split conduction or valence bands appear to be ideal systems for studying MO effects, as they have a rather simple spin-dependent multiband scheme. However, these systems have rarely been investigated up to now, mainly because they usually show a very weak Rashba spin splitting (RSS) which cannot be resolved experimentally, and also because RSS had been found only in the two-dimensional electron-gas or metallic systems formed at the surface or interface where the MO effect is hardly detectable.

This situation has been greatly improved recently by the discovery of the giant *bulk* RSS in the polar semiconductor BiTeI. Angle-resolved photoemission spectroscopy [8] has revealed that the bulk conduction bands in BiTeI are subject to a large RSS [see Fig. 1(a)], well described by the 2D Rashba Hamiltonian $H_R = \mathbf{p}^2/2m + \lambda \mathbf{e}_z \cdot (\mathbf{S} \times \mathbf{p})$, near the time-reversal symmetry point A, where $\mathbf{e}_z$ is the direction of the potential gradient breaking the inversion symmetry, and $\mathbf{S}$ and $\mathbf{p}$ are the spin and momentum operators, respectively. This leads to a Dirac-conelike band dispersion near $\mathbf{p} = \mathbf{0}$. The succeeding first-principles calculations [9,10] and the optical conductivity spectra [11] further revealed that not only the bottom conduction bands (BCBs) but also the top valence bands (TVBs) are subject to a comparable RSS in BiTeI. This condition allows several distinct interband and intraband transitions between these two sets of states. The reduced dimensionality together with RSS introduces a well-defined singularity in the joint density of states at the band edge. Therefore, this material is a promising candidate to host the enhanced spin-charge coupling and/or the magnetoelectric effect with the possible applications to spintronics. From this viewpoint, the MO effect is an intriguing issue in BiTeI; the interplay between RSS and external magnetic field has been extensively investigated from theoretical side [12–15] but hardly ever probed experimentally in a real compound. Of particular interest are the states near the

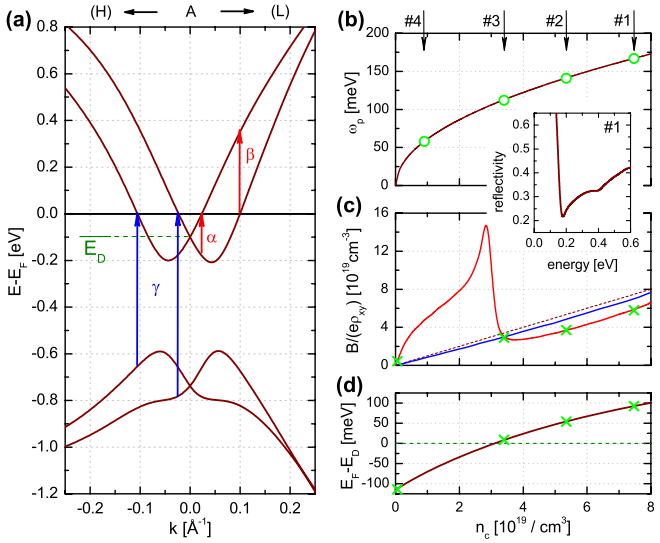

FIG. 1 (color online). (a) Calculated electronic band structure of BiTeI with the α, β (intraband), and γ (interband) transitions for a given Fermi level E_F. E_D depicts the position of the Dirac point. Carrier densities determined (b) from the plasma frequency (circles) and (c) from the Hall response (crosses). See the related discussion in the text. Vertical arrows indicate the samples investigated experimentally, while red (light), blue (dark), and dashed curves of panel (c) represent the calculated Hall response with or without taking into account SOI, and the conventional relation $R_H = -1/(n_c e)$, respectively. The inset of panel (b) shows the measured low-temperature reflectivity of sample no. 1. (d) Fermi level as a function of the carrier concentration n_c.

band-crossing (Dirac) point formed by RSS, as they turn into novel Landau levels under magnetic field similar to the case of graphene [12]. Thus, it is important to know their impact on the MO response, e.g., by tuning the Fermi level E_F across the Dirac point. In this Letter, we accordingly study the MO properties of BiTeI both experimentally and theoretically. It is shown that due to giant RSS of bulk bands, the material exhibits large MO effect in the infrared spectra under moderate magnetic fields up to 3 T. This enhancement is anticipated to be even more pronounced in the low-energy region near the Dirac point of BCBs.

BiTeI has a trigonal crystal structure with C_{3v} symmetry composed of consecutive Bi, Te, and I layers stacking along the c axis of the crystal [8,9]. Because of ionicity and covalency of Bi–I and Bi–Te bonds, respectively, the bulk material possesses an intrinsic polarity along the c axis which, when coupled with the strong atomic SOI of Bi, leads to a huge bulk RSS. The calculated band structure of BCBs and TVBs around the band gap (along the $H - A - L$ direction), together with the possible interband and intraband transitions, is shown in Fig. 1(a).

We discuss the MO effects in terms of the off-diagonal components of the optical conductivity tensor. First the reflectivity spectra were measured over a broad energy range ($E = 10$ meV $-$ 40 eV and $E = 10$ meV $-$ 6 eV at room and low temperatures, respectively) and the σ_{xx} diagonal component of the conductivity tensor was obtained by the Kramers-Kronig transformation. As the second step, the complex MO Kerr angle spectra, $\Phi_K(\omega)$, were measured over the photon energy region of 80–550 meV by combining a Fourier-transform infrared spectrometer, a polarization modulation technique [16,17], and a 3 T room temperature-bore magnet. The off-diagonal conductivity σ_{xy} was derived via the following relation:

$$\Phi_K = \theta_K + i\eta_K = -\frac{\sigma_{xy}}{\sigma_{xx}\sqrt{1 + (4\pi i/\omega)\sigma_{xx}}}. \quad (1)$$

All the experiments were carried out in reflection configuration with nearly normal incidence on cleaved surfaces of the optically isotropic ab plane. The low-temperature study was performed at $T = 10$ K. The MO experiments were done in a polar geometry; i.e., external magnetic fields in the range of $B = \pm 3$ T have been applied perpendicular to the sample surface (see Supplemental Material [18]).

From the theoretical side, the longitudinal conductivity σ_{xx} has been derived from the Kubo formula as described in Ref. [11], while the transverse conductivity σ_{xy} has been calculated to linear order in the external magnetic field B using the Fukuyama formula [19],

$$\begin{aligned}\sigma_{xy}(i\omega_\ell) = B\frac{e^3\hbar}{2\omega}k_B T\sum_n \frac{1}{V}\sum_{\mathbf{k}}\{m\mathrm{Tr}[G_- v_x G v_x G \\ - G_- v_x G_- v_x G] + m^4\mathrm{Tr}[G_- v_y G_- v_x G v_x G v_y \\ - G_- v_x G_- v_x G v_y G v_y + v_x G v_y G_- v_x G_- v_y G_- \\ - v_x G v_y G_- v_y G_- v_x G_- + G_- v_x G v_x G v_y G v_y \\ - G_- v_x G v_y G v_x G v_y]\}, \quad (2)\end{aligned}$$

where $G = [i\tilde{\epsilon}_n + E_F - H]^{-1}$ is the one-particle thermal Green's function, $\tilde{\epsilon}_n = \epsilon_n + \frac{\Gamma}{2}\mathrm{sgn}(\epsilon_n)$ with $\epsilon_n = (2n+1)\pi k_B T$, Γ the damping constant, and G_- is obtained from G by replacing $\epsilon_n \to \epsilon_n + \omega_\ell$ with $\omega_\ell = 2\ell\pi k_B T$; m denotes the electron mass, V the volume of the system, and v_i $(i = x, y)$ the velocity operator represented in matrix form as

$$v_{i,nm} = \langle n|v_i(\mathbf{k})|m\rangle = \frac{1}{\hbar}\langle n|\frac{\partial H(\mathbf{k})}{\partial k_i}|m\rangle, \quad (3)$$

where $|n\rangle$ corresponds to the nth eigenstate of $H(\mathbf{k})$. These matrix elements were computed by downfolding the *ab initio* Hamiltonian [20] to a low-energy tight binding model, which was constructed for the 12 valence and 6 conduction bands around the band gap [9]. To evaluate the formula (2), the sum over Matsubara frequencies was transformed into a contour integral along the branch cuts of the Green's functions [21]. After performing the analytic continuation $i\omega_\ell \to \omega$, the contour integral as well as the $\mathbf{k}$ momentum integral were evaluated numerically. Γ was fixed at 12.8 meV for the

calculation of both the diagonal and the off-diagonal conductivity spectrum.

The carrier densities n_c of different samples were first estimated from the plasma edge of the free carriers in the *ab* plane [depicted in the inset of Fig. 1(b)] using $\sqrt{n_c e^2/(m^* \epsilon_0 \epsilon_\infty)}$, where m^* is the effective carrier mass, and ϵ_∞ the high-frequency (background) dielectric constant as determined by angle-resolved photoemission spectroscopy and optical measurements, respectively [8,11]. The effect of carrier doping may be treated within the rigid band approximation and then the carrier concentration dependence of the Fermi energy shows a monotonic behavior as plotted in Fig. 1(d). To study the effect of carrier doping on MO response, we targeted the samples with representative carrier concentrations, whose E_F are above (samples no. 1 and 2), around (no. 3), and below (no. 4) the Dirac point. High-quality single crystals were grown by the chemical vapor transport method and n_c was controlled by the growth conditions for samples nos. 1 and 3. On the other hand, the Bridgman method has been employed as described in Ref. [8] for samples nos. 2 and 4, and n_c has been tuned by doping Sb and Cu, respectively. As indicated in Fig. 1(b) the corresponding carrier densities estimated from the plasma frequencies are $n_c \simeq 7.5$, 5.4, 3.4, and $0.9 \times 10^{19}/\mathrm{cm}^3$ for samples nos. 1–4, respectively.

Dc Hall effect measurements are commonly used as an alternative way to determine the carrier concentration. However, the simple relation $R_H = -1/(n_c e)$, which applies for materials with only one type of charge carriers (single band model), does not hold in BiTeI with Rashba-split bands. Correspondingly, Fig. 1(c) shows the calculated dc Hall response as a function of n_c with and without taking into account SOI, which clearly demonstrates that the conventional Hall data analysis under(over)estimates the carrier density above (below) the Dirac point. The origin of the large enhancement of B/ρ_{xy} (or the suppression of R_H) around the Dirac point is due to the coexistence of electron and hole pockets, or equivalently because of the donutlike shape of the Fermi surface formed by the Rashba-split conduction bands. For samples nos. 1–3 the results of magnetotransport experiments in conjunction with the calculations give the carrier density values n_c in accord with the values estimated from the plasma edge [Fig. 1(b)]. However, this is not the case for sample no. 4, where the complex characteristics of the Fermi surface makes the simple estimate based on the plasma frequency less adequate. Consequently, in the following analysis we use $n_c \simeq 0.06 \times 10^{19}/\mathrm{cm}^3$ as the carrier density of sample no. 4 estimated from the realistic band structure model.

The measured diagonal and off-diagonal optical conductivity spectra for sample no. 1 (with E_F well above the Dirac point) are plotted in Fig. 2. Our theoretical results, also shown in Fig. 2, closely reproduce the experimentally observed $\sigma_{xx}(\omega)$ and $\sigma_{xy}(\omega)$ spectra in both magnitude and energy position. Two distinct features in the MO response are

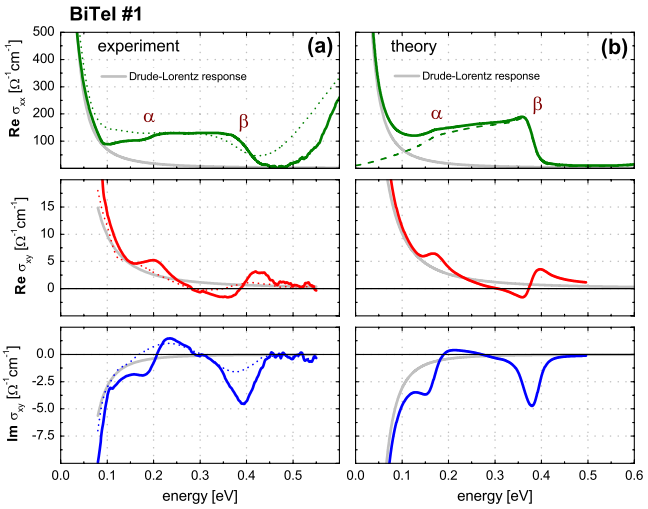

FIG. 2 (color online). Comparison between the diagonal and off-diagonal optical conductivity spectra obtained experimentally (left panels) and theoretically (right panels) for sample no. 1 at 10 K. Spectra measured at room temperature are also plotted with dotted lines. Colored (dark) lines represent the actual curves, while gray (light) ones illustrate the contribution of the Drude-Lorentz response estimated by fitting the low energy part of the experimental σ_{xx} spectrum (see the text for details). As the calculation of σ_{xx} (dashed line in the top right panel) does not cover the free carrier excitations, the Drude part has been added manually according to the fit for easy comparison.

discerned in the $\sigma_{xy}(\omega)$ spectra around 0.2 and 0.4 eV, in addition to a Drude-Lorentz response dominating the region below 0.1 eV. These two resonance structures well correspond to the intraband transitions α and β [see Fig. 1(a)] assigned in the $\sigma_{xx}(\omega)$ spectra [11]. The observed MO response (up to $\pm 5\ \Omega^{-1}\,\mathrm{cm}^{-1}$ at 0.1–0.5 eV) at 3 T is remarkably large for such a nonmagnetic system. For a comparison, the interband contribution to the transverse conductivity for typical nonmagnetic semiconductors indium antimonide, indium arsenide, germanium, or gallium aresenide at 3 T is of the order of 0.01–0.3 $\Omega^{-1}\,\mathrm{cm}^{-1}$ as calculated from the Faraday rotation [22]. Even in the case of the ferromagnetic $(Gd_{0.95}Ca_{0.05})_2Mo_2O_7$, the MO signal in the 0.1–1 eV energy range governed by the Mo $4d$ intraband transitions is an order of magnitude smaller, and only the spin chirality induced contribution present in $Nd_2Mo_2O_7$ is comparable with the present system [23]. The observed MO activity at 3 T can well compare with the typical magnitude of the MO response (σ_{xy}) coming from the $p - d$ charge-transfer excitations in oxide ferromagnets [23,24]. We also emphasize here that the MO response of BiTeI is still remarkable at room temperature, as it is weaker only by a factor of 2.5 compared to 10 K (see left panels of Fig. 2).

In BiTeI, because of RSS of BCBs and TVBs, the optical transitions between initial and final states having opposite spin directions are allowed. In the presence of external magnetic field, the probability of these transitions becomes different when induced by right or left circularly polarized

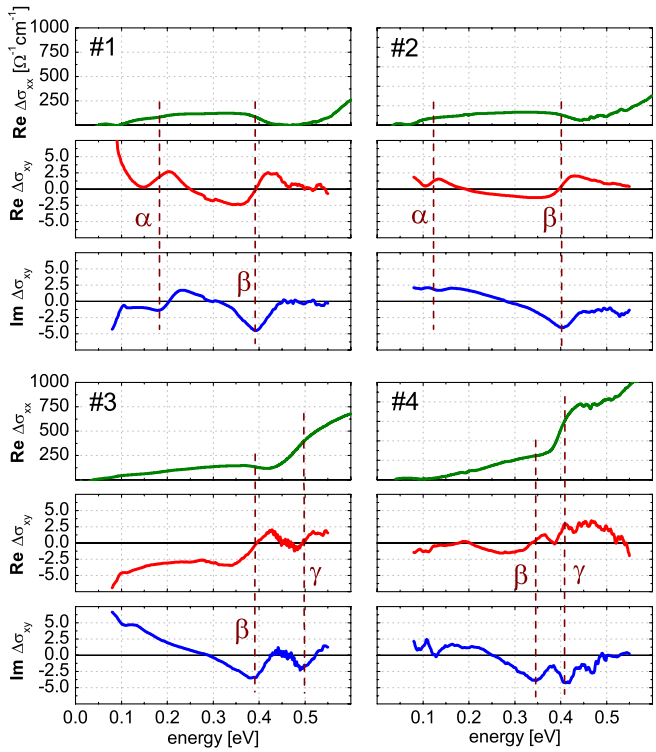

FIG. 3 (color online). Systematics of spectral features in the low-temperature optical conductivity with changing the Fermi energy E_F. E_F decreases monotonically from sample no. 1 towards sample no. 4, crossing the Dirac point near sample no. 3. Broken lines represent the positions of the structures identified with the intra- (α and β) and interband (γ) transitions.

photons, which is represented by σ_{xy} and is the common origin of MO effects such as the magneto-circular dichroism, the Faraday and the MO Kerr effects. As the magnitude of these MO phenomena scales linearly with the strength of the SOI [25], the large MO response of BiTeI is a direct consequence of the gigantic bulk RSS in this material. This is an astonishing effect of the SOI, because the magnetization of BiTeI at $B = 3$ T is merely of the order of 10^{-4} μ_B/Bi [26], several orders of magnitude smaller than the spontaneous magnetization in the ferromagnets mentioned above.

To have a better insight into the consequences of RSS on the MO properties, the contribution of free carrier excitations has been subtracted by assuming a simple Drude model expressed with use of the cyclotron frequency $\omega_c = eB/m^*$, and the relaxation time $\tau = \hbar/\Gamma$. The dc conductivity $\sigma_{xx}(\omega = 0, B = 0)$ was determined from the transport experiments, then τ, the only free parameter, was chosen so as to fit the low-energy part of the experimental diagonal conductivity spectra. The corresponding Drude-Lorentz curves are also depicted in Fig. 2. Figure 3 shows the resulting spectra of σ_{xx} and σ_{xy}, whose Drude-Lorentz components are subtracted with the similar analysis, for all the samples investigated. The values of the effective mass ($m^* = 0.18$ m$_0$) and the damping constant obtained from these fits are in good agreement with those found

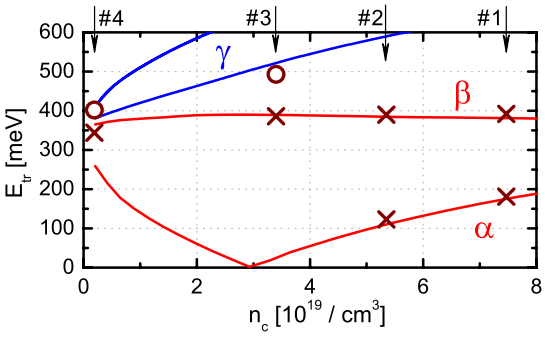

FIG. 4 (color online). Energy position (E_{tr}) of intra- and interband transitions in BiTeI with changing carrier density (n_c) as assigned on the basis of the experimental (symbols) and theoretical (solid lines) MO spectra. Crosses and open circles correspond to the features identified with the intra- and interband transitions, respectively.

by angle-resolved photoemission spectroscopy [8] as well as those used for the aforementioned theoretical model.

Next, we study the evolution of different spectral features found in the MO response with varying carrier densities. Starting with sample no. 1, in the $\sigma_{xx}(\omega)$ spectrum one can identify the characteristic features of the intraband transitions, namely the vertical transitions to (from) the Fermi level E_F as depicted by α (β) in Fig. 1(a). The Zeeman splitting induced by magnetic fields in the range of 3 T is small compared to RSS, nevertheless the transition probability for intraband excitations becomes different for left and right circularly polarized lights. The dispersive line shape found in the real part of $\sigma_{xy}(\omega)$ supports this scenario [27], giving a clear evidence for the strong SOI in BiTeI. Lowering E_F to the level of sample no. 2, the α band shifts toward lower energy with decreasing magnitude, while the β band remains at almost the same position. Further variation of E_F (as in samples nos. 3 and 4) causes slight shifts of β as well, while α is no more discernable in the measured frequency range. On the other hand, the spectral feature corresponding to the edge of the interband transitions γ [see Fig. 1(a)] enters into the detectable window from higher energies for samples nos. 3 and 4, observed as a sharp rise in $\sigma_{xx}(\omega)$ and as the band with dispersive line shape in $\sigma_{xy}(\omega)$. Figure 4 shows the calculated and observed results for the relevant transition energies as a function of carrier density n_c. The agreement between the experimental results and the theoretical predictions is excellent in the case of α and β intraband transitions, and reasonably good for the γ interband transitions.

To summarize, we have studied the MO response of BiTeI with a large RSS by systematically changing the position of the Fermi level around the band-crossing (Dirac) point. Besides its crucial role in the spin-dependent band splitting in the vicinity of the Fermi energy, SOI allows the otherwise prohibited spin-flop transitions between these bands. Given that BiTeI is a nonmagnetic system, the observed MO effect arising from the intraband

transitions is found to be huge compared with conventional (spin degenerate) semiconductors. Our theoretical model can quantitatively account for the experimental results and also predict the significant impact of the Dirac point on the dc Hall effect.

This research is supported by MEXT Grants No. 19048008, No. 19048015, No. 20740167, No. 24224009, and No. 24244054, Strategic International Cooperative Program (Joint Research Type) from Japan Science and Technology Agency, by the Japan Society for the Promotion of Science (JSPS) through its "Funding Program for World-Leading Innovative R&D on Science and Technology (FIRST Program)," the DFG Research Unit FOR 723, as well as by Hungarian Research Funds with reference No. OTKA PD75615, No. CNK80991, No. Bolyai 00256/08/11, and No. TÁMOP-4.2.2.B-10/12010-0009. We gratefully acknowledge computing resources provided by bwGRiD [28], member of the German D-Grid initiative, funded by the Ministry for Education and Research (Bundesministerium für Bildung und Forschung) and the Ministry for Science, Research and Arts Baden-Württemberg (Ministerium für Wissenschaft, Forschung und Kunst Baden-Württemberg). G. A. H. S. acknowledges support from MEXT and DAAD.

*ldemko@dept.phy.bme.hu

†Present address: Department of Photonics and Applied Physics, Gwangju Institute of Science and Technology, Gwangju 500-712, Korea.

[1] D. Awschalom and N. Samarth, Physics **2**, 50 (2009).

[2] S. D. Bader and S. S. P. Parkin, Annu. Rev. Condens. Matter Phys. **1**, 71 (2010).

[3] J. Sinova and I. Žutić, Nature Mater. **11**, 368 (2012).

[4] R. Winkler, *Spin Orbit Coupling Effects in Two-Dimensional Electron and Hole Systems*, Springer Tracts in Modern Physics, Vol. 191 (Springer, Berlin, 2003).

[5] S. Murakami, N. Nagaosa, and S.-C. Zhang, Science **301**, 1348 (2003).

[6] S. D. Ganichev, E. L. Ivchenko, V. V. Bel'kov, S. A. Tarasenko, M. Sollinger, D. Weiss, W. Wegscheider, and W. Prettl, Nature (London) **417**, 153 (2002).

[7] K. H. Bennemann, J. Magn. Magn. Mater. **200**, 679 (1999).

[8] K. Ishizaka *et al.*, Nature Mater. **10**, 521 (2011).

[9] M. S. Bahramy, R. Arita, and N. Nagaosa, Phys. Rev. B **84**, 041202(R) (2011).

[10] M. S. Bahramy, B.-J. Yang, R. Arita, and N. Nagaosa, Nature Commun. **3**, 679 (2012).

[11] J. S. Lee, G. A. H. Schober, M. S. Bahramy, H. Murakawa, Y. Onose, R. Arita, N. Nagaosa, and Y. Tokura, Phys. Rev. Lett. **107**, 117401 (2011).

[12] S.-Q. Shen, M. Ma, X. C. Xie, and F. C. Zhang, Phys. Rev. Lett. **92**, 256603 (2004).

[13] A. A. Burkov and L. Balents, Phys. Rev. B **69**, 245312 (2004).

[14] W. Xu, C. H. Yang, and J. Zhang, Appl. Phys. Lett. **91**, 221911 (2007).

[15] M. S. Kushwaha, Phys. Rev. B **74**, 045304 (2006).

[16] K. Sato, Jpn. J. Appl. Phys. **20**, 2403 (1981).

[17] K. Ohgushi, Y. Okimoto, T. Ogasawara, S. Miyasaka, and Y. Tokura, J. Phys. Soc. Jpn. **77**, 034713 (2008).

[18] See Supplemental Material at http://link.aps.org/supplemental/10.1103/PhysRevLett.109.167401 for more details on the experimental methods and analyses of Kerr angle spectra.

[19] H. Fukuyama, Prog. Theor. Phys. **42**, 1284 (1969).

[20] Details of *ab inito* calculations can be found in Ref. [9].

[21] G. D. Mahan, *Many-Particle Physics* (Plenum, New York, 2000), 3rd ed.

[22] L. M. Roth, Phys. Rev. **133**, A542 (1964).

[23] I. Kézsmárki, S. Onoda, Y. Taguchi, T. Ogasawara, M. Matsubara, S. Iguchi, N. Hanasaki, N. Nagaosa, and Y. Tokura, Phys. Rev. B **72**, 094427 (2005).

[24] Z. Fang, N. Nagaosa, K. S. Takahashi, A. Asamitsu, R. Mathieu, T. Ogasawara, H. Yamada, M. Kawasaki, Y. Tokura, and K. Terakura, Science **302**, 92 (2003).

[25] P. M. Oppeneer, T. Maurer, J. Sticht, and J. Kübler, Phys. Rev. B **45**, 10924 (1992).

[26] G. A. H. Schober, H. Murakawa, M. S. Bahramy, R. Arita, Y. Kaneko, Y. Tokura, and N. Nagaosa, Phys. Rev. Lett. **108**, 247208 (2012).

[27] S. Wittekoek, T. J. A. Popma, J. M. Robertson, and P. F. Bongers, Phys. Rev. B **12**, 2777 (1975).

[28] http://www.bw-grid.de.